Bone Reports 20 (2024) 101745

Contents lists available at ScienceDirect

Bone Reports

journal homepage: www.elsevier.com/locate/bonr

Microvascular disease not type 2 diabetes is associated with increased cortical porosity: A study of cortical bone microstructure and intracortical vessel characteristics

Maximilian T. Löffler [a,b,c,*,1], Po-hung Wu [a,1], Amir M. Pirmoazen [a], Gabby B. Joseph [a], Jay M. Stewart [d], Isra Saeed [a], Jing Liu [a], Anne L. Schafer [e,f], Ann V. Schwartz [f], Thomas M. Link [a], Galateia J. Kazakia [a]

[a] Department of Radiology and Biomedical Imaging, University of California, 185 Berry St, Suite 350, San Francisco, CA 94107, USA
[b] Department of Diagnostic and Interventional Radiology, University Medical Center Freiburg, Freiburg im Breisgau, Germany
[c] Department of Diagnostic and Interventional Neuroradiology, School of Medicine, Klinikum rechts der Isar, Technical University of Munich, Munich, Germany
[d] Department of Ophthalmology, University of California, San Francisco, CA, USA
[e] Department of Medicine, University of California, San Francisco, CA, USA
[f] Department of Epidemiology and Biostatistics, University of California, San Francisco, CA, USA

ARTICLE INFO

Keywords:
Cortical bone
Porosity
Type 2 diabetes
Microvascular disease
Dynamic contrast-enhanced MRI
HR-pQCT

ABSTRACT

Introduction: Fracture risk is elevated in type 2 diabetes (T2D) despite normal or even high bone mineral density (BMD). Microvascular disease (MVD) is a diabetic complication, but also associated with other diseases, for example chronic kidney disease. We hypothesize that increased fracture risk in T2D could be due to increased cortical porosity (Ct.Po) driven by expansion of the vascular network in MVD. The purpose of this study was to investigate associations of T2D and MVD with cortical microstructure and intracortical vessel parameters.

Methods: The study group consisted of 75 participants (38 with T2D and 37 without T2D). High-resolution peripheral quantitative CT (HR-pQCT) and dynamic contrast-enhanced MRI (DCE-MRI) of the ultra-distal tibia were performed to assess cortical bone and intracortical vessels (outcomes). MVD was defined as ≥1 manifestation including neuropathy, nephropathy, or retinopathy based on clinical exams in all participants. Adjusted means of outcomes were compared between groups with/without T2D or between participants with/without MVD in both groups using linear regression models adjusting for age, sex, BMI, and T2D as applicable.

Results: MVD was found in 21 (55 %) participants with T2D and in 9 (24 %) participants without T2D. In T2D, cortical pore diameter (Ct.Po.Dm) and diameter distribution (Ct.Po.Dm.SD) were significantly higher by 14.6 μm (3.6 %, 95 % confidence interval [CI]: 2.70, 26.5 μm, $p = 0.017$) and by 8.73 μm (4.8 %, CI: 0.79, 16.7 μm, $p = 0.032$), respectively. In MVD, but not in T2D, cortical porosity was significantly higher by 2.25 % (relative increase = 12.9 %, CI: 0.53, 3.97 %, $p = 0.011$) and cortical BMD (Ct.BMD) was significantly lower by −43.6 mg/cm^3 (2.6 %, CI: −77.4, −9.81 mg/cm^3, $p = 0.012$). In T2D, vessel volume and vessel diameter were significantly higher by 0.02 mm^3 (13.3 %, CI: 0.004, 0.04 mm^3, $p = 0.017$) and 15.4 μm (2.9 %, CI: 0.42, 30.4 μm, $p = 0.044$), respectively. In MVD, vessel density was significantly higher by 0.11 mm^{-3} (17.8 %, CI: 0.01, 0.21 mm^{-3}, $p = 0.033$) and vessel volume and diameter were significantly lower by −0.02 mm^3 (13.7 %, CI: −0.04, −0.004 mm^3, $p = 0.015$) and − 14.6 μm (2.8 %, CI: −29.1, −0.11 μm, $p = 0.048$), respectively.

Conclusions: The presence of MVD, rather than T2D, was associated with increased cortical porosity. Increased porosity in MVD was coupled with a larger number of smaller vessels, which could indicate upregulation of neovascularization triggered by ischemia. It is unclear why higher variability and average diameters of pores in T2D were accompanied by larger vessels.

* Corresponding author at: Department of Radiology and Biomedical Imaging, University of California, 185 Berry St, Suite 350, San Francisco, CA 94107, USA.
E-mail address: m_loeffler@web.de (M.T. Löffler).
[1] Authors contributed equally.

https://doi.org/10.1016/j.bonr.2024.101745
Received 17 August 2023; Received in revised form 5 December 2023; Accepted 22 February 2024
Available online 25 February 2024

1. Introduction

Type 2 diabetes (T2D) is a global health burden with approximately 462 million persons affected worldwide in 2017 and high prevalence, particularly in developed countries (Khan et al., 2020). T2D is characterized by hyperglycemia that can lead to micro- and macrovascular complications; of those, retinopathy, nephropathy, neuropathy can be summarized as microvascular disease (MVD) (Khosla et al., 2021). MVD is also associated with other diseases that affect bone, such as chronic kidney disease (CKD) and alcoholism for example. Skeletal fragility has been recently acknowledged as a diabetic complication in addition to these vascular complications. While BMD is preserved or even increased in T2D (Bonds et al., 2006; Ma et al., 2012), evidence indicates that bone structure and material properties may be altered and thus could lead to increased fracture risk (Napoli et al., 2017). A proposed structural alteration associated with T2D is increased cortical porosity (Ct.Po), which is strongly associated with decreased bone strength (McCalden et al., 1993) and independently predicts fracture risk, as shown in postmenopausal women without diabetes (Bala et al., 2014). The largest cohort study to date reported higher Ct.Po. with T2D but only at the tibia, not the radius (Samelson et al., 2018). Other smaller studies have found increased porosity in T2D at the radius (Burghardt et al., 2010a) or the tibia (Farr et al., 2014; Shanbhogue et al., 2016) or at neither location (Patsch et al., 2013). Some results suggest that increased cortical porosity is primarily found in T2D with MVD, which could explain the inconsistent results (Shanbhogue et al., 2016; Samakkarnthai et al., 2020). Recently, Samakkarnthai et at. found higher Ct.Po in the tibia in T2D patients with clinically significant peripheral vascular disease (assessed using transcutaneous oxygen tension) compared to controls (Samakkarnthai et al., 2020).

Apparent density of cortical bone contributes approximately 4 times exponentially more to bone stiffness compared to apparent density of trabecular bone (Schaffler and Burr, 1988), which motivates our particular interest in Ct.Po. Understanding the biological drivers of pathological pore development is key to prevention and treatment strategies. Furthermore, fracture risk assessment can be improved by a deeper understanding of the pathomechanisms behind skeletal fragility in T2D. Increased Ct.Po is introduced by a remodeling imbalance upon intracortical canals and the endocortical surface lining as typically seen in Menopause (Ramchand and Seeman, 2018). Previous imaging studies have advanced the knowledge, but – so far – no study has been able to elucidate the biological mechanisms driving Ct.Po. The vascular system, as one of the primary contents of pore space (Garita et al., 2021), could be involved in a pathological process that leads to pore expansion. This process would require resorption of cortical bone for vascular canals.

Combining dynamic contrast-enhanced MRI (DCE-MRI) data with HR-pQCT data, we have previously developed a multimodal imaging technique to visualize vessel-filled pores within cortical bone in the tibia (Wu et al., 2019). We applied this multimodal imaging technique to the distal tibia of participants with and without T2D, who were examined for presence of MVD. We hypothesize that ambiguous results for Ct.Po in T2D patients are due to heterogeneous prevalence of MVD in this population. The purpose of this study was to investigate the relationship of T2D and MVD with cortical microstructure and intracortical vessel characteristics, both assessed in the same anatomic location. Insofar, we aimed to test the assumptions that

1) T2D is associated with cortical bone/vessel parameters or
2) MVD is associated with cortical bone/vessel parameters independent of T2D status.

2. Materials and methods

2.1. Study participants

All study participants were enrolled as part of an ongoing longitudinal study starting in 2017 that investigates the progression and etiology of Ct.Po in diabetic bone disease. This study represents a cross-section at baseline of this cohort that is followed for 5 years. This HIPAA compliant study was approved by the UC San Francisco (UCSF) institutional review board (study number: 16-20196). All participants gave written informed consent. The study's sample size was calculated based on preliminary data for longitudinal change in Ct.Po in T2D and age- and sex-matched healthy controls ($n = 20$ subjects per group required to detect a significantly greater increase in Ct.Po in T2D vs. control with a power of 93 % and $\alpha = 0.05$). Participants were recruited from the community, primarily through flyers posted in primary care clinics, or from the UCSF diabetes clinic (only participants with T2D). Participants with T2D were exposure-matched by frequency of age and sex to participants without diabetes. Enrollment was concluded with $n = 38$ in the T2D group and n = 38 matched participants without diabetes to account for possible drop-out and to allow detection of changes in sub-groups. After participants passed initial eligibility screening all clinical exams and imaging procedures were performed within a 2-week period. Clinical data including height and weight to calculate body mass index (BMI), current blood tests for creatinine and glycated hemoglobin (HbA1c), and information about use of diabetes medications were collected. Glomerular filtration rate (GFR) was estimated using the Chronic Kidney Disease Epidemiology Collaboration (CKD-EPI) formula.

We included postmenopausal women and men with an age of 50–70 years and a bone mineral density of $0 \geq$ T-score > -2.5 assessed by DXA ($n = 20$ subjects excluded after eligibility screening with DXA). We excluded older subjects because at this age there is a significant increase of osteoporosis-related cortical bone loss. Likewise, we wanted to exclude osteoporotic subjects (T-score ≤ -2.5). Participants with T2D had a diagnosis for >3 years as defined by the American Diabetes Association, which includes either receiving pharmacological treatment for 3 or more years or HbA1c of ≥6.5 for 3 or more years in the case of no pharmacological treatment (only diet control). We excluded persons with a history of metabolic bone disease or intake of bone active drugs including bisphosphonates or teriparatide (no use in the last year or for >12 months ever), calcitonin or thiazolidinedione (current use), prednisolone >5 mg per day or the equivalent glucocorticoid for >10 days in the last 3 months, and thyroid hormone replacement with current thyroid stimulating hormone (TSH) <0.1 mIU/l. Furthermore, patients with chronic gastrointestinal disease (including inflammatory bowel disease, celiac disease, or other malabsorptive disease including short-gut syndrome), hepatic impairment (known cirrhosis or if transaminase levels 3-fold above normal limit), or persons with current alcohol consumption >3 drinks/day, current illicit drug use, trauma or surgery near radius or tibia imaging sites, and with immobilization for >1 week in the previous 6 months were excluded. Additionally, all participants were required to have an estimated GFR ≥40 ml/min/1.73 m^2 and no conditions that precluded undergoing MRI (including BMI >40 kg/m^2 as these subjects will exceed weight and size limitations of the MRI scanner).

2.2. Clinical examination of vascular health

All participants were clinically examined for presence of neuropathy, nephropathy, and retinopathy. Examiners were blinded to the T2D status of participants. For assessment of neuropathy, the 10 g Semmes-Weinstein monofilament and a 128 Hz tuning fork were used to evaluate the perception of vibration and loss of protective sensation, respectively. The monofilament and tuning fork were applied at the first to fifth metatarsal head and first phalanx, and the tuning fork was additionally applied to the medial malleolus of both feet. Loss of perception/sensation at ≥1 site was defined as neuropathy. Nephropathy was evaluated analyzing a spot urine sample. Urine albumin-to-creatinine ratio ≥ 30 μg/mg was considered increased urinary albumin excretion, a marker for the development of nephropathy (American Diabetes Association, 2013). A board-certified expert ophthalmologist (JMS) assessed the presence/extent of retinopathy in fundus

photographs (Maamari et al., 2014). Non-proliferative and proliferative diabetic retinopathy were summarized as diabetic retinopathy. MVD was defined as presence of at least one organ manifestation (skin sensation, eye, or kidney).

2.3. High-resolution peripheral quantitative computed tomography

HR-pQCT of the ultra-distal tibia was performed using a XtremeCT scanner (Scanco Medical AG, Brüttisellen, Switzerland). The scan protocol was set to the manufacturer's standard in-vivo parameters (tube voltage 60 kVp, tube current 900 mA, isotropic nominal resolution 82 μm, exposure 3 μSv per scan). The non-dominant lower leg was scanned with a fixed scan region starting 37.5 mm proximal to the joint line and extending 9.02 mm proximally (110 slices). The contralateral side was scanned if participants reported a history of fracture on the non-dominant leg. The root mean square coefficient of variation (RMSCV) values of HR-pQCT outcomes are <1.4 % for densitometric parameters and 1.3 % to 8.9 % for structural parameters (Bonaretti et al., 2017). Image quality was evaluated for motion artifacts immediately after acquisition using the manufacturer's qualitative grading scheme (Pialat et al., 2012) to ensure adequate quality (grades 1 to 3). Acquisition was repeated if necessary to achieve adequate quality.

The cortical bone compartment was segmented using a semi-automated three-step algorithm implemented in a customized image processing language (IPL v.506a-ucsf, Scanco Medical AG) (Burghardt et al., 2010b). First, the periosteal and endosteal cortical boundaries were identified in an auto-contouring process and manually corrected if necessary. Then, pores within the cortical compartment were located. Finally, the cortical bone and the pore mask were combined into a final mask of the cortical compartment including pores. This mask was used to extract cortical bone parameters from HR-pQCT scans that comprised cortical thickness (Ct.Th, mm), cortical bone mineral density (Ct.BMD, mg HA/cm^3), mean cortical pore diameter (Ct.Po.Dm, μm), cortical pore diameter distribution (Ct.Po.Dm.SD, μm), total cortical pore volume (Ct.Po.V, mm^3), and cortical porosity (Ct.Po, unitless ratio %).

Ct.Po.V, Ct.Po.Dm and Ct.Po.Dm.SD are direct voxel-based measures of the integral volume, average diameter and standard deviation (=diameter distribution) of the intracortical pores, whereas Ct.Po is a relative voxel-based measure of the volume of the intracortical pore space (=void volume) normalized by the sum of the pore and cortical bone volume (Burghardt et al., 2010b). Intracortical void volume that can be captured by HR-pQCT is considered to represent larger Haversian canals given that resolution is limited to approximately 100 μm. Least significant detectable change (calculated based on the root mean square coefficient of variation for repeat measurements) was 0.05 mm for Ct.Th, 14 mg HA/cm^3 for Ct.BMD, 22 μm for Ct.Po.Dm, 17 μm for Ct.Po.Dm.SD, and 0.92 for Ct.Po in a population of 27 women with mean age 61 years (Burghardt et al., 2010b).

2.4. Dynamic contrast-enhanced magnetic resonance imaging

Cortical pore content was assessed by DCE-MRI (Wu et al., 2019) performed on a clinical 3 T Discovery MR750w scanner (GE Healthcare, Waukesha, WI, USA) using a sixteen-channel flex coil (In-Vivo Corporation, Gainesville, FL, USA). Scan field-of-view (FOV) covered the ultra-distal HR-pQCT scan location, which centered 34.5 mm proximal from the tibiotarsal joint line. A 3D scan time series was acquired over 9 min using a spoiled gradient-recalled (SPGR) sequence with circular cartesian under sampling (CIRCUS) for increased temporal resolution of 30 s (TR/TE 11.8–12.2 ms/4.1 ms, bandwidth ±125 kHz, flip angle 20°, FOV 12 × 9 cm^2, matrix size 512 × 384, in-plane resolution 230 × 230 μm^2, and total of 56 slices with thickness of 500 μm) (Liu et al., 2016). Intravenous gadolinium-based contrast agent (Gadavist, Bayer Healthcare, Whippany, NJ, USA) was injected with a volume adapted to body weight (0.1 ml/kg) at a flow rate of 2 ml/s and 1 min delay after the start of the acquisition.

2.5. Multimodal intracortical vessel detection

Image analysis for calculation of vessel metrics was performed using a previously described in-house developed multi-step procedure including both DCE-MRI and HR-pQCT images (Wu et al., 2019). In brief, boundaries of the cortical compartment as well as intracortical pores were identified on HR-pQCT. DCE-MRI images at each time point were separately registered to the ultra-distal scan region of HR-pQCT by rigid transformation using FSL (Analysis Group, FMRIB, Oxford, UK) followed by modified demons registration (Vercauteren et al., 2009) to account for distortions in MRI images. Temporal smoothing was applied to registered MRI to reduce effects of mis-registration and MRI time series were normalized to the average of the first two scans. A Frangi filter was applied to the time series to enhance vessel structures (Frangi et al., 1998). To detect voxels representing vessels within the cortical compartment, 4 features in the enhancement curve were analyzed including the first component of principal component analysis (PCA), area under the curve (AUC), standard deviation of temporal intensity, and summation of absolute temporal intensity difference (SATID). All voxels within cortical bone were clustered using a 2-stage hierarchical k-means algorithm based on these 4 features (Arthur and Vassilvitskii, 2006). Finally, a vessel connection algorithm was implemented to fill in discontinuities in the vessel mask (Wu et al., 2019).

Vessel metrics that were extracted from DCE-MRI scans within the cortical bone compartment comprised vessel density (average vessel count per cortical bone volume, 1/mm^3), average vessel volume (mm^3), average vessel diameter (μm), vessel-pore ratio (ratio of total vessel count to total pore number, unitless ratio %), and vessel-pore volume fraction (ratio of total vessel volume to total pore volume, unitless ratio in %). Using this imaging technique tubular structures of 250 μm diameter could be measured with almost perfect accuracy (volume overlap ratio ~ 1), while diameters of 200 μm still showed fair overlap in a virtual phantom (Wu et al., 2019). Given this resolution smaller nutrient arteries in cortical bone could be visualized before they branch into smaller arterioles and even smaller capillaries contained within Haversian canals (Löffler et al., n.d.).

2.6. Statistics

Statistical analyses were performed using IBM SPSS Statistics 28 (IBM, Armonk, NY) and the extension PROCESS v4.2 for moderation analysis (Hayes, 2022). Level of statistical significance was set at $p < 0.05$ for all tests. Proportions of categorical variables were compared using chi-square tests (i.e., sex, race, MVD manifestations). Means of population characteristics (ie, age, BMI, HbA1c, albumin-to-creatinine ratio) and means of outcomes (ie, Ct.Po, Ct.Po.V, Ct.Po.Dm, Ct.Po.Dm.SD, Ct.Th, Ct.BMD, vessel density, avg. vessel volume, avg. vessel diameter, vessel-pore ratio) were compared using student's *t*-tests. Moreover, means of outcomes were compared using linear regression models adjusting for age, sex, and BMI, because these are factors known to influence bone outcomes (Cooper et al., 2007). 95 % confidence intervals (CIs) of differences in means were calculated. Our assumptions were tested in a stepwise approach. First, outcomes were compared between participants with and without T2D. Second, outcomes were compared between participants with and without MVD additionally adjusting for T2D status (to remove any effects of MVD on outcomes by a pathway through T2D). No correction for multiple comparisons to control Type I error rate was performed as we considered this study exploratory.

Sensitivity analyses were performed on the subgroup of participants with T2D: 1) with adjustment for the use of diabetes medication, and 2) after excluding participants with CKD defined by a GFR <60 ml/min/1.73 m^2. Prior to the analysis in the subgroup of participants with T2D we ascertained the absence of a significant risk-difference modification by T2D on the effect of MVD on outcomes (Rothman et al., 2008). We adjusted only for the use of diabetes medications that have a known

effect on bone (Glucagon-like peptide-1 [GLP-1] receptor agonists, Dipeptidyl peptidase 4 [DPP-4] inhibitors, and insulin) (Elamir et al., 2020). Of those, only GLP-1 receptor agonists showed a significant influence on the models, but we decided not to include these results because there were only $n = 3$ participants using GLP-1 agonists.

3. Results

The study group consisted of a total of 75 participants (41 women) with a mean age of 61.8 ± 5.4 years. Of those, 38 were T2D participants and 37 were participants without diabetes. One participant without diabetes was excluded from analysis because of prediabetes (5.7 % < HbA1c < 6.4 %). Vessel metrics of one participant without diabetes could not be analyzed due to motion artifacts in the DCE-MRI images. Participants with T2D had significantly higher HbA1c and BMI than participants without diabetes (both $p < 0.05$). We found stage 3 A (GFR 45–59) CKD in four participants with T2D, of those, one had MVD. Overall, 30 participants (41 %) showed signs of MVD including 21 participants with T2D (55 %) and 9 participants without diabetes (24 %). Only two participants without diabetes had single intraretinal hemorrhages in the far peripheral retina that, as such, could not clearly be attributed to MVD and were regarded as incidental findings. Demographics and more details about manifestations of MVD in the study groups are shown in Table 1.

Table 1
Characteristics of study population stratified by T2D status.

	All (n = 75)	T2D (n = 38)	No T2D (n = 37)	T2D vs. no T2D, p-value
Women, n (%)	41 (55 %)	20 (53 %)	21 (57 %)	0.720
Race, n (%)				0.314
• White or Caucasian	47 (63 %)	21 (55 %)	26 (70 %)	0.179
• Asian	21 (28 %)	12 (32 %)	9 (24 %)	0.484
• Black or African American	5 (7 %)	4 (11 %)	1 (3 %)	0.174
• Hawaiian or other pacific islander	1 (1 %)	1 (3 %)	0	–
• Other non-white	1 (1 %)	0	1 (3 %)	–
Age, years, mean ± SD	61.8 ± 5.4	61.5 ± 5.6	62.0 ± 5.4	0.639
BMI, kg/m^2, mean ± SD	26.6 ± 4.3	28.1 ± 4.1	25.1 ± 3.9	**0.002**
Duration of T2D, years, mean ± SD	–	11.3 ± 7.6	–	–
HbA1c, %, median (IQR)	5.7 (1.7)	6.95 (1.3)	5.3 (0.3)	**<0.001**
Glomerular filtration rate, mL/min/1.73 m^2, mean ± SD	88.3 ± 16.7	85.3 ± 14.9	91.4 ± 18.0	0.109
Albumin-creatinine ratio, %, median (IQR)	8 (15)	12 (31)	4 (5)	0.979
Microvascular disease, n (%)	30 (40 %)	21 (55 %)	9 (24 %)	**0.024**
• Neuropathy	12 (16 %)	5 (13 %)	7 (19 %)	–
• Nephropathy	10 (13 %)	8 (21 %)	2 (5 %)	–
• Retinopathy	4 (5 %)	4 (11 %)	0	–
• Neuropathy and retinopathy	1 (1 %)	1 (3 %)	0	–
• Nephropathy and retinopathy	1 (1 %)	1 (3 %)	0	–
• Neuropathy, nephropathy, and retinopathy	2 (3 %)	2 (5 %)	0	–

Statistically significant p-values are in bold. BMI = body mass index, HbA1c = hemoglobin A1c.

3.1. HR-pQCT cortical bone parameters

Cortical bone parameters stratified by T2D status and the presence of MVD are depicted in Fig. 1 and shown in Supplemental Table 1 and 2, respectively. In a model adjusted for age, sex, and BMI, mean Ct.Po.Dm and Ct.Po.Dm.SD were significantly increased by 14.6 mm (3.6 %, CI: 2.70, 26.5 mm, $p = 0.017$) and 8.73 mm (4.8 %, CI: 16.7, 0.79 mm, $p = 0.032$), respectively, in T2D participants compared to participants without diabetes. There was no significant difference between T2D and participants without diabetes for Ct.Po, Ct.Po.V, Ct.Th, and Ct.BMD. In contrast, in a model adjusted for age, sex, BMI, and T2D status, mean Ct.Po and Ct.Po.V were significantly increased by 2.25 % (relative increase = 12.9 %, CI: 0.53, 3.97 %, $p = 0.011$) and 24.2 mm^3 (12.2 %, CI: 2.32, 46.1 mm^3, $p = 0.031$), respectively, in participants with MVD compared to those without. Mean Ct.BMD was significantly decreased by −43.6 mg/cm^3 (2.6 %, CI: −77.4, −9.81 mg/cm^3, $p = 0.012$) in MVD. There was no significant difference between participants with MVD and those without for Ct.Po.Dm, Ct.Po.Dm.SD, and Ct.Th. Investigating only the subgroup of T2D participants there were no significant differences between those with/without MVD for any bone parameters (Supplemental Table 5). However, numerical differences showed the same directionality as for the entire group. After excluding participants with CKD ($n = 4$) all differences between participants with/without T2D (Ct.Po.Dm and Ct.Po.Dm.SD) and between participants with/without MVD (Ct.Po, Ct.Po.V, and Ct.BMD) remained statistically significant.

3.2. DCE-MRI intracortical vessel metrics

Vessel metrics stratified by T2D status and the presence of MVD are depicted in Fig. 2 and shown in Supplemental Table 3 and 4, respectively. In a model adjusted for age, sex, and BMI, mean vessel volume and vessel diameter were significantly increased by 0.02 mm^3 (13.3 %, CI: 0.004, 0.04 mm^3, $p = 0.017$) and 15.4 μm (2.9 %, CI: 0.42, 30.4 μm, $p = 0.044$), respectively, in T2D participants compared to participants without diabetes (Fig. 3). There was no significant difference between T2D participants and participants without diabetes for vessel density and vessel-pore ratio. In contrast, in a model adjusted for age, sex, BMI, and T2D status, mean vessel density was significantly increased by 0.11 mm^{-3} (17.8 %, CI: 0.01, 0.21 mm^{-3}, $p = 0.033$) in participants with MVD compared to those without (Figs. 3 and 4). Mean vessel volume and diameter were significantly decreased by −0.02 mm^3 (13.7 %, CI: −0.04, −0.004 mm^3, $p = 0.014$) and by −14.6 μm (2.8 %, CI: −29.1, −0.11 μm, $p = 0.048$), respectively, in MVD. Investigating only the subgroup of participants with T2D, significance was not reached for differences between those with/without MVD for any vessel parameters (Supplemental Table 5). However, numerical differences showed the same directionality as for the entire group. After excluding participants with CKD ($n = 4$) no significant differences in intracortical vessel metrics remained between participants with/without T2D or with/without MVD, respectively.

4. Discussion

In this study, cortical bone and intracortical vessel metrics were assessed at the tibia and compared between participants with and without T2D and with and without MVD, adjusting for age, sex, and BMI. We found T2D not to be associated with cortical porosity or intracortical vessel density. Instead, MVD was associated with higher cortical porosity and higher vessel density.

The relationship between Ct.Po and MVD is in line with current evidence. A previous study found lower Ct.BMD, lower Ct.Th, and higher Ct.Po in the radius as well as a tendency towards higher Ct.Po in the tibia in subjects with T2D and MVD compared to healthy controls without diabetes (Shanbhogue et al., 2016). Moreover, T2D patients with transcutaneous oxygen tension ≤40 mmHg as a marker for MVD had significantly higher Ct.Po in the distal tibia compared to controls

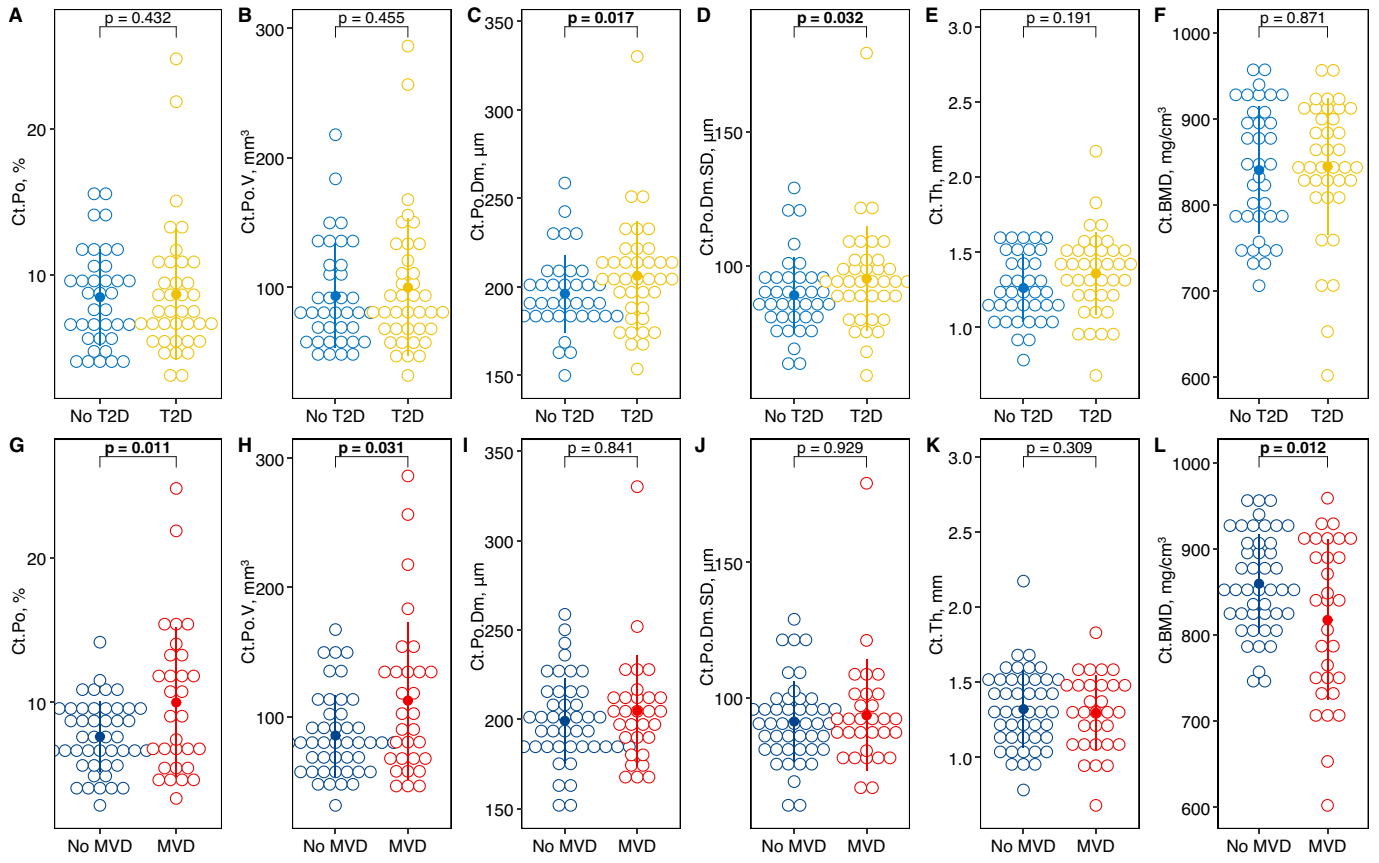

Fig. 1. Dot plots with means and standard deviations (dot and line) of HR-pQCT parameters stratified by T2D status (A-F) or presence of MVD (G-L). *P*-values are from linear regression models adjusting for age, sex, and BMI in models comparing participants with/without T2D and, additionally, adjusting for T2D status in models comparing participants with/without MVD.

(Samakkarnthai et al., 2020). A study of subjects with type 1 diabetes described higher Ct.Po in the tibia, but not in the radius, in the presence of neuropathy – one manifestation of MVD (Vilaca et al., 2021). Sensitivity analysis in the subgroup of T2D participants in this study showed similar tendencies for associations between MVD and Ct.Po, Ct.Po.V, and Ct.BMD, but they did not reach statistical significance presumably due to low statistical power. After excluding participants with mild CKD ($n = 4$, 1 with MVD / 3 without MVD) differences between participants with and without MVD remained significant (Ct.Po, Ct.Po.V, and Ct.BMD). CKD increases cortical porosity and fracture risk (McNerny and Nickolas, 2017). Due to the detrimental effects of CKD on cortical bone, the higher incidence of CKD in the non-MVD group may have masked an even larger effect of MVD on porosity. Moreover, we observed a mean HbA1c of 6.95 % in participants with T2D. In a similar way, good glycemic control in T2D could have masked more severe effects on bone vasculature and cortical properties. There are hints that cortical porosity in T2D is particularly increased in some patients (Wölfel et al., 2020). In line with these observations, we found two participants with T2D and MVD who showed approximately two-fold increased Ct.Po and Ct.Po.V compared to all other participants.

Studies of cortical bone in T2D that did not evaluate MVD found more ambiguous results. In 1069 participants of the Framingham study, T2D was associated with lower Ct.BMD and higher Ct.Po in the tibia, but not in the radius (Samelson et al., 2018). A study of 18 T2D patients and 18 age- and height-matched controls found a >2-fold increase in Ct.Po in the radius, but no other significant differences in cortical bone measures in the radius or tibia (Burghardt et al., 2010a). In an expanded study of 80 women, the same group found significant deficits in cortical microstructural and biomechanical parameters in participants with T2D and a history of fragility fracture compared to those with T2D and no history of fragility fracture. They found no significant differences in cortical parameters between participants with T2D and matched controls without diabetes (Patsch et al., 2013).

In contrast to the results found for MVD, T2D was associated with significantly increased Ct.Po.Dm but not Ct.Po.V or Ct.Po. Due to limited resolution, cortical pores assessed by HR-pQCT are considered to represent the largest pores including Haversian canals (Burghardt et al., 2010b). Ct.Po is the ratio of void volume (pores) to total cortical volume. If Ct.Po remains unchanged despite a significant increase in Ct.Po.Dm, as we found in the T2D group, the geometry of the Haversian network must change, which could imply a coalescence of canals. Clustering and increased pore size may play a major role in the etiology of fractures through the development of stress concentrations (Jordan et al., 2000) and due to the strong association between pore clustering and reduced cortical bone fracture toughness (Granke et al., 2016). We speculate that an increase in average pore diameter contributes more to fracture risk than an increase in relative void volume (=Ct.Po) because larger pores lead to stress concentrations and accelerated crack propagation and therefore reduced fracture toughness (Zimmermann et al., 2011).

To the best of our knowledge, this is the first in-vivo study specifically addressing the relationship between MVD and alterations of cortical bone in T2D. We employed DCE-MRI, a unique imaging technique that enables the study of cortical bone beyond the morphologic and densitometric parameters of HR-pQCT (Wu et al., 2019). DCE-MRI uses contrast enhancement characteristics to identify and assess intracortical vessels. The distinction between cortical pore metrics and intracortical vessel metrics is important because cortical porosity, even in the mid-cortical and periosteal regions of the cortex, can contain adiposity rather than – or in addition to – vasculature (Garita et al., 2021; Wu et al., 2019; Goldenstein et al., 2010). We found higher

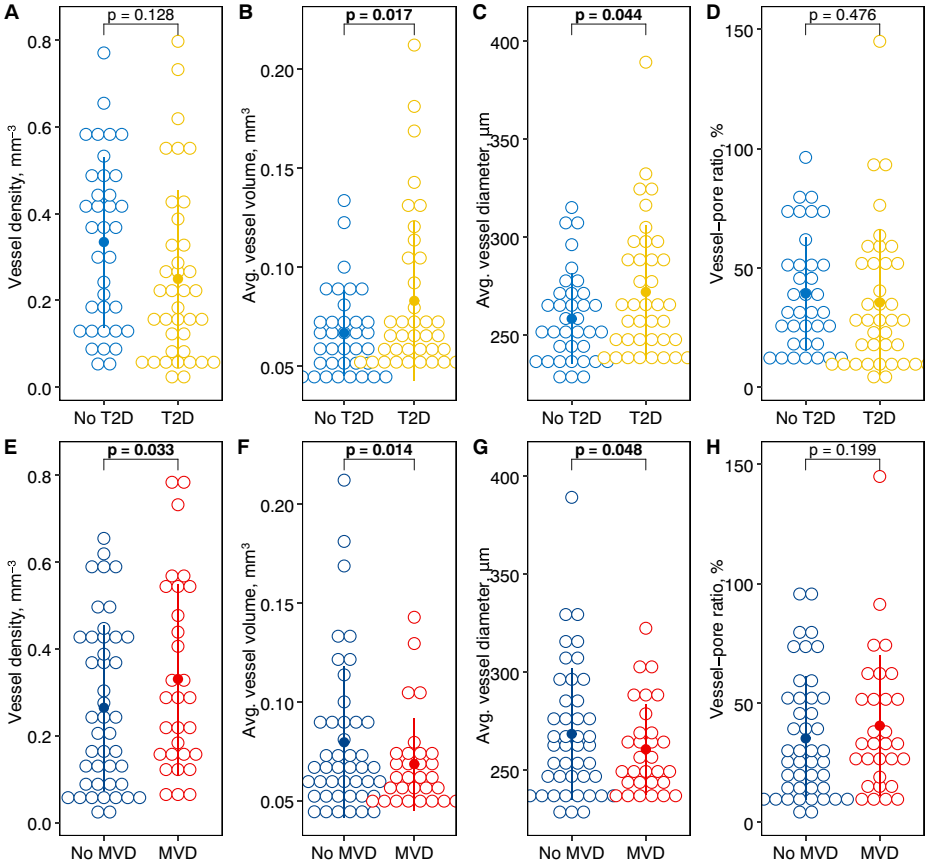

Fig. 2. Dot plots with means and standard deviations (dot and line) of intracortical vessel metrics assessed by DCE-MRI and stratified by T2D status (A-D) or presence of MVD (E-F). *P*-values are from linear regression models adjusting for age, sex, and BMI in models comparing participants with/without T2D and, additionally, adjusting for T2D status in models comparing participants with/without MVD.

average vessel volume and diameter in T2D. In participants with MVD, in contrast, higher vessel density was accompanied by lower average vessel volume and diameter. Sensitivity analysis exploring the association between MVD and vessel metrics in the subgroup of participants with T2D supported this finding with similar point estimates, although associations did not reach statistical significance. Excluding participants with mild CKD led to similar point estimates of differences in intracortical vessel metrics based on the T2D status and the presence of MVD. Again, these differences did not reach statistical significance.

Of note, there were some outliers as well as an overlap of values between participants with and without T2D for bone and vessel parameters. In sensitivity analyses where outliers were removed all findings remained significant (at $p < 0.05$) except for the difference in average vessel diameter between participants with and without T2D. The effect of T2D on vasculature and bone likely involves other factors that moderate or mediate outcome values.

In diabetic MVD, microvascular dysfunction is triggered by sustained hyperglycemia via multiple biochemical pathways and leads to irreversible damage in different organs (Barrett et al., 2017). MVD is a systemic disease where one organ manifestation can be sentinel to injury in other organs. The link between microvascular dysfunction and diabetic bone disease is unclear. Decreased skeletal blood supply could potentially affect bone remodeling in a way that favors bone resorption over bone formation (Hofbauer et al., 2022). In an earlier stage of T2D, hyperglycemia has not yet led to microvascular damage that can be captured in clinical exams (as performed in this study). We observed larger intracortical vessels associated with T2D in a heterogeneous group where 55 % of T2D participants showed signs of MVD (model not accounting for MVD). Microaneurysms represent the earliest clinically visible changes of diabetic retinopathy. Similarly, enlargement or ectasia of intracortical vessels could be a hallmark of early diabetic bone disease. In a later stage of the disease with clinically manifest MVD, we found increased Ct.Po and a large number of small vessels as seen in neovascularization triggered by ischemia. In line with this notion, decreased microvascular blood flow assessed using transcutaneous oxygen tension was associated with increased Ct.Po in subjects with T2D (Samakkarnthai et al., 2020).

This study has limitations. First, in-vivo imaging is limited in resolution. HR-pQCT can only resolve pores of approximately 100 µm in diameter and larger (Nirody et al., 2015). However, these largest pores are the most biomechanically relevant when investigating potential causes for increased fracture risk on the micro-meter scale (Zimmermann et al., 2011). Moreover, increased Ct.Po in participants with MVD concurred with decreased Ct.BMD, which is a parameter highly correlated with small scale cortical porosity as measured by micro-CT (Ostertag et al., 2014). Of note, the new generation HR-pQCT (Xtreme CT II, Scanco Medical, Brüttisellen, Switzerland) provides nominal resolution of 61 µm. DCE-MRI can only reliably detect vessels of ~230 µm diameter or larger. Therefore, the average vessel diameter, particularly in MVD, represents only the largest vessels. Nevertheless, significant differences in vessel diameter were observed between groups. Whether these differences equally translate to vessels at a smaller scale remains unclear. We assume that the vessels identified in our scans of the ultra-distal tibia are non-sinusoidal. The morphology and column-like arrangement (see Figs. 3 and. 4) shows strong similarity to metaphyseal microvessels in the murine skeletal system that plays an important role in angiogenesis and osteogenesis (Kusumbe et al., 2014). Second, due to study design, we were not able to compare balanced groups of subjects with and without MVD. Violation of the assumption of homogeneity of variances affects Type I error rates, particularly when

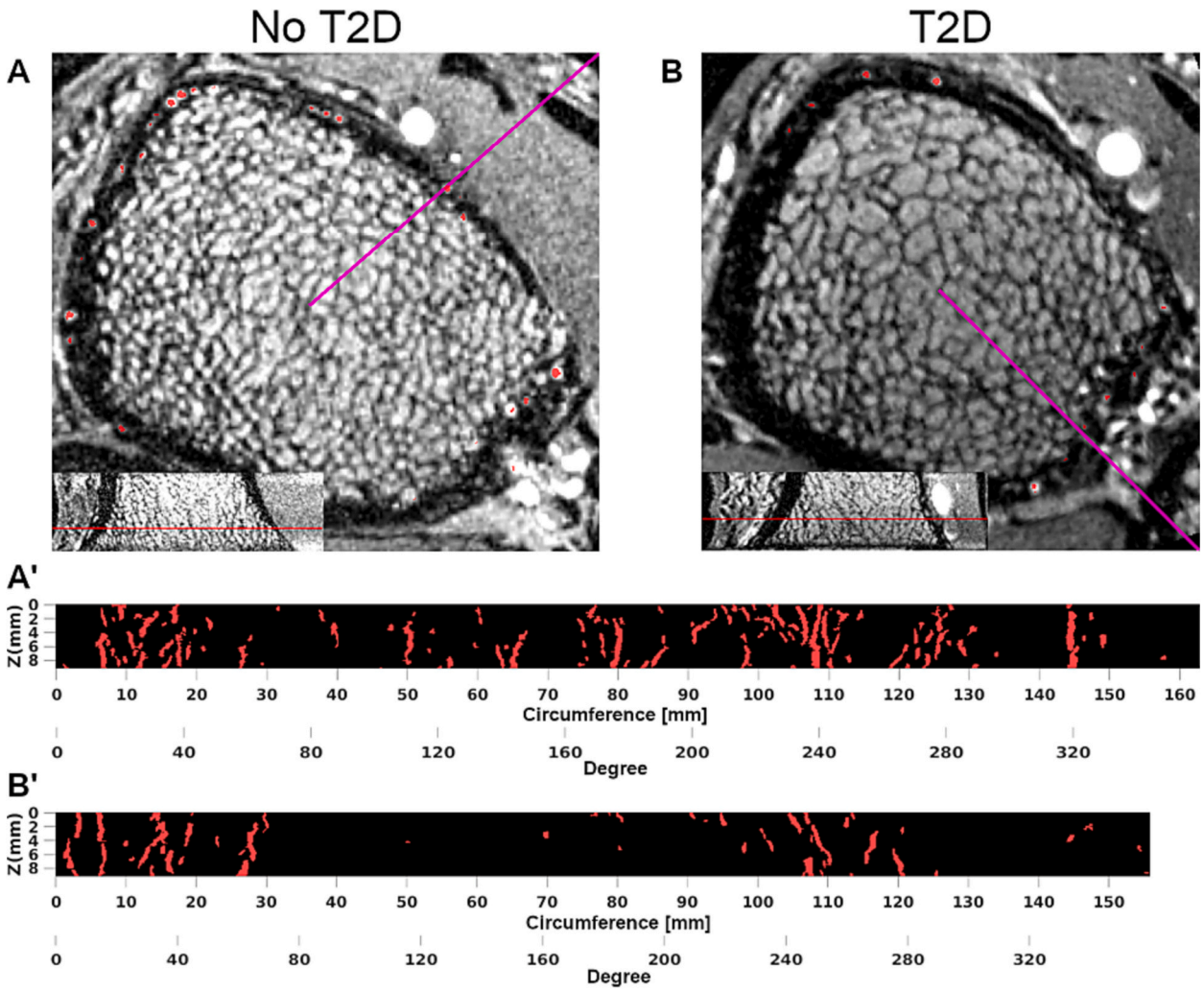

Fig. 3. DCE-MRI of ultra-distal tibia of a 70-year-old man without diabetes (A and A') and of a 56-year-old man with T2D (B and B′). Neither participant showed any clinical signs of MVD. Red voxels in axial views (A and B) represent detected intracortical vessels. Radial maximum intensity projections (MIPs, A' and B′) show metaphyseal vessels in column-like arrangement. Purple lines in axial views represent circumference origins of MIPs. Resolution is limited to larger diameter (>230 μm) vessels. The participant with T2D had fewer and on average larger intracortical vessels compared to the participant without diabetes.

groups sizes are unequal. To control Type I error rates, we reran all linear regression models using bootstrapping with 2000 samples as a robust method to estimate confidence intervals (Efron and Tibshirani, 1994). All statistically significant differences were confirmed except for the differences of average vessel diameter using this alternative test method and a p-level of <0.05. Furthermore, there is a chance of Type I errors due to multiple comparisons that we did not correct for in this exploratory study. Third, MVD can develop due to conditions other than diabetes mellitus and MVD was found in a quarter of participants without T2D. Whether manifestations of MVD without underlying T2D share the same pathomechanisms affecting bone as observed in diabetic MVD is unclear. Diabetic MVD can manifest in different organs and at different times. Since MVD affects the whole body, we grouped participants with evidence of MVD in at least one of the examined organs (eye, kidney, and peripheral nervous system). In the peripheral nervous system a variety of mechanisms are hypothesized that may affect bone, one of those being neurovascular regulation of bone modelling and remodeling (Beeve et al., 2019), which could be influenced by MVD regardless of underlying T2D. Of note, negative monofilament and vibration assessment using a tuning fork might not be sufficient to exclude neuropathy. Therefore, diagnosis of neuropathy could be underestimated, especially in participants with T2D. However, we found a 19 % prevalence of neuropathy in participants without diabetes that was higher than expected (around 8 % in people older than 55 years (*Neurology*, 1995)) and could represent a sampling error due to a high prevalence of non-diabetic peripheral neuropathies (e.g., caused by vitamin B12 deficiency, alcoholism, disc herniations, or peripheral vascular disease) (Pop-Busui et al., 2017). Fourth, since we excluded persons older than 70 years and with osteoporotic bone density, our results cannot be generalized to this population of high fracture risk.

5. Conclusions

This study showed that MVD was associated with higher cortical porosity, higher intracortical vessel density, and smaller intracortical vessels. In contrast, T2D, independent of MVD, was associated with larger cortical pore diameter, as well as lower intracortical vessel density and larger intracortical vessels. These findings in T2D could represent an intermediate stage of impaired bone remodeling due to hyperglycemia that subsequently manifests in higher cortical porosity in parallel with clinically apparent MVD. Microstructural changes associated with both conditions – T2D and MVD – may be characteristic of diabetic bone disease and lead to decreased bone strength.

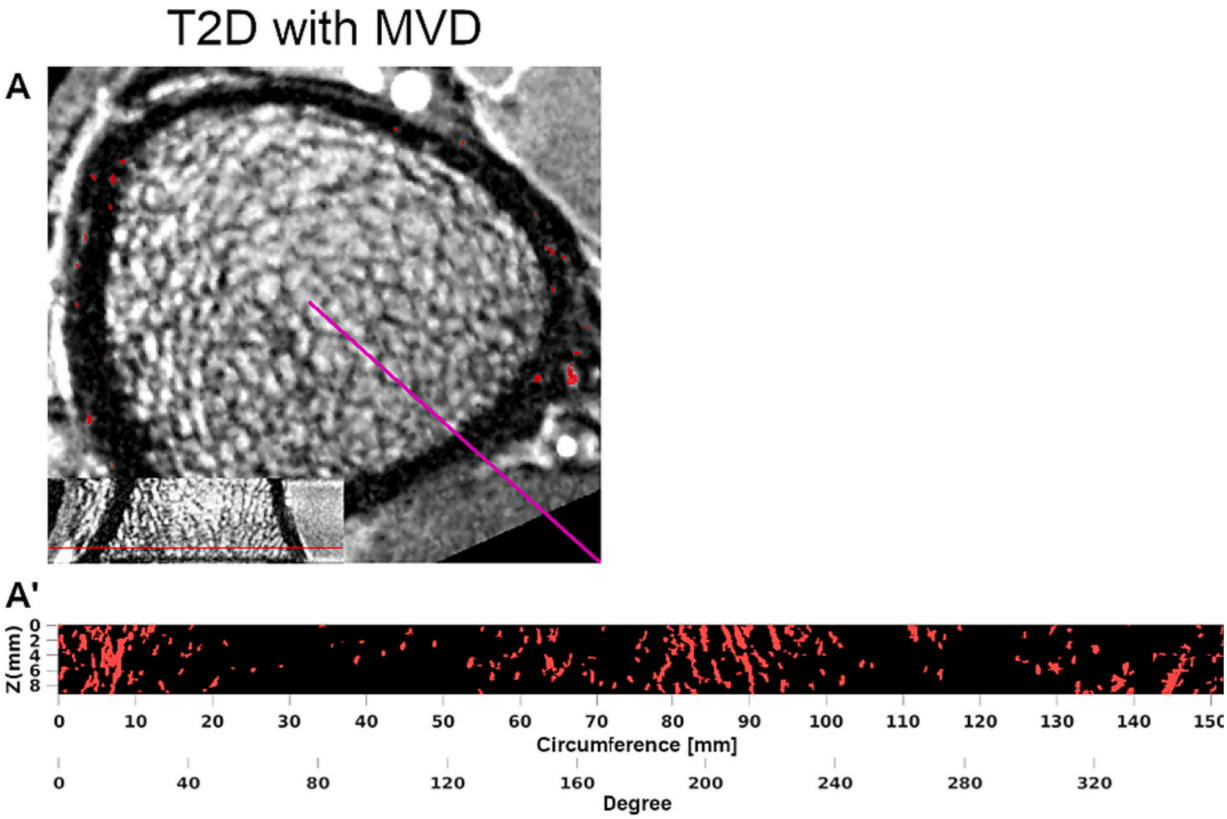

Fig. 4. DCE-MRI of ultra-distal tibia of a 59-year-old female T2D participant with neuropathy and proliferative diabetic retinopathy. Red voxels in axial view (A) and radial MIP (A') represent detected intracortical vessels. This T2D participant with MVD had relatively more and smaller intracortical vessels compared to a healthy control (Fig. 3). See legend of Fig. 3 for more details on image creation.

CRediT authorship contribution statement

Maximilian T. Löffler: Writing – review & editing, Writing – original draft, Visualization, Validation, Software, Resources, Methodology, Investigation, Formal analysis, Data curation, Conceptualization. **Pohung Wu:** Visualization, Validation, Software, Methodology, Investigation, Formal analysis, Conceptualization. **Amir M. Pirmoazen:** Investigation, Data curation. **Gabby B. Joseph:** Writing – review & editing, Formal analysis. **Jay M. Stewart:** Investigation. **Isra Saeed:** Project administration, Investigation. **Jing Liu:** Methodology. **Ann V. Schwartz:** Writing – review & editing, Conceptualization. **Thomas M. Link:** Writing – review & editing, Resources, Conceptualization. **Galateia J. Kazakia:** Writing – review & editing, Validation, Supervision, Resources, Methodology, Funding acquisition, Data curation, Conceptualization.

Declaration of competing interest

The authors declare the following financial interests/personal relationships which may be considered as potential competing interests:

Galateia J. Kazakia reports financial support was provided by the National Institutes of Health.

Data availability

Data will be made available on request.

Acknowledgments

This work was supported by the National Institutes of Health – National Institute of Arthritis and Musculoskeletal and Skin Diseases [grant numbers R01AR069670, R03AR064004, R01AR076159].

Appendix A. Supplementary data

Supplementary data to this article can be found online at https://doi.org/10.1016/j.bonr.2024.101745.

References

American Diabetes Association, 2013. Standards of medical care in diabetes—2013. Diabetes Care 36 (Suppl. 1), S11–S66. https://doi.org/10.2337/dc13-S011.

Arthur, D., Vassilvitskii, S., 2006. k-means++: The Advantages of Careful Seeding. http://ilpubs.stanford.edu:8090/778/ (accessed September 18, 2022).

Bala, Y., Zebaze, R., Ghasem-Zadeh, A., Atkinson, E.J., Iuliano, S., Peterson, J.M., Amin, S., Bjørnerem, Å., Melton, L.J., Johansson, H., Kanis, J.A., Khosla, S., Seeman, E., 2014. Cortical porosity identifies women with osteopenia at increased risk for forearm fractures. J. Bone Miner. Res. Off. J. Am. Soc. Bone Miner. Res. 29, 1356–1362. https://doi.org/10.1002/jbmr.2167.

Barrett, E.J., Liu, Z., Khamaisi, M., King, G.L., Klein, R., Klein, B.E.K., Hughes, T.M., Craft, S., Freedman, B.I., Bowden, D.W., Vinik, A.I., Casellini, C.M., 2017. Diabetic microvascular disease: an Endocrine Society scientific statement. J. Clin. Endocrinol. Metab. 102, 4343–4410. https://doi.org/10.1210/jc.2017-01922.

Beeve, A.T., Brazill, J.M., Scheller, E.L., 2019. Peripheral neuropathy as a component of skeletal disease in diabetes. Curr. Osteoporos. Rep. 17, 256–269. https://doi.org/10.1007/s11914-019-00528-8.

Bonaretti, S., Vilayphiou, N., Chan, C.M., Yu, A., Nishiyama, K., Liu, D., Boutroy, S., Ghasem-Zadeh, A., Boyd, S.K., Chapurlat, R., McKay, H., Shane, E., Bouxsein, M.L., Black, D.M., Majumdar, S., Orwoll, E.S., Lang, T.F., Khosla, S., Burghardt, A.J., 2017. Operator variability in scan positioning is a major component of HR-pQCT precision error and is reduced by standardized training. Osteoporos. Int. J. Establ. Result Coop. Eur. Found. Osteoporos. Natl. Osteoporos. Found. USA. 28, 245–257. https://doi.org/10.1007/s00198-016-3705-5.

Bonds, D.E., Larson, J.C., Schwartz, A.V., Strotmeyer, E.S., Robbins, J., Rodriguez, B.L., Johnson, K.C., Margolis, K.L., 2006. Risk of fracture in women with type 2 diabetes: the Women's Health Initiative Observational Study. J. Clin. Endocrinol. Metab. 91, 3404–3410. https://doi.org/10.1210/jc.2006-0614.

Burghardt, A.J., Issever, A.S., Schwartz, A.V., Davis, K.A., Masharani, U., Majumdar, S., Link, T.M., 2010a. High-resolution peripheral quantitative computed tomographic imaging of cortical and trabecular bone microarchitecture in patients with type 2 diabetes mellitus. J. Clin. Endocrinol. Metab. 95, 5045–5055. https://doi.org/10.1210/jc.2010-0226.

Burghardt, A.J., Buie, H.R., Laib, A., Majumdar, S., Boyd, S.K., 2010b. Reproducibility of direct quantitative measures of cortical bone microarchitecture of the distal radius and tibia by HR-pQCT. Bone 47, 519–528. https://doi.org/10.1016/j.bone.2010.05.034.

Cooper, D.M.L., Thomas, C.D.L., Clement, J.G., Turinsky, A.L., Sensen, C.W., Hallgrímsson, B., 2007. Age-dependent change in the 3D structure of cortical porosity at the human femoral midshaft. Bone 40, 957–965. https://doi.org/10.1016/j.bone.2006.11.011.

Efron, B., Tibshirani, R.J., 1994. An Introduction to the Bootstrap. Chapman and Hall/CRC, New York. https://doi.org/10.1201/9780429246593.

Elamir, Y., Gianakos, A.L., Lane, J.M., Sharma, A., Grist, W.P., Liporace, F.A., Yoon, R.S., 2020. The effects of diabetes and diabetic medications on bone health. J. Orthop. Trauma 34, e102–e108. https://doi.org/10.1097/BOT.0000000000001635.

Farr, J.N., Drake, M.T., Amin, S., Melton, L.J., McCready, L.K., Khosla, S., 2014. In vivo assessment of bone quality in postmenopausal women with type 2 diabetes. J. Bone Miner. Res. Off. J. Am. Soc. Bone Miner. Res. 29, 787–795. https://doi.org/10.1002/jbmr.2106.

Frangi, A.F., Niessen, W.J., Vincken, K.L., Viergever, M.A., 1998. Multiscale vessel enhancement filtering. In: Wells, W.M., Colchester, A., Delp, S. (Eds.), Med. Image Comput. Comput.-Assist. Interv. — MICCAI'98. Springer, Berlin, Heidelberg, pp. 130–137. https://doi.org/10.1007/BFb0056195.

Garita, B., Maligro, J., Sadoughi, S., Wu, P.H., Liebenberg, E., Horvai, A., Link, T.M., Kazakia, G.J., 2021. Microstructural abnormalities are evident by histology but not HR-pQCT at the periosteal cortex of the human tibia under CVD and T2D conditions. Med. Nov. Technol. Devices. 10, 100062 https://doi.org/10.1016/j.medntd.2021.100062.

Goldenstein, J., Kazakia, G., Majumdar, S., 2010. In vivo evaluation of the presence of bone marrow in cortical porosity in postmenopausal osteopenic women. Ann. Biomed. Eng. 38, 235–246. https://doi.org/10.1007/s10439-009-9850-7.

Granke, M., Makowski, A.J., Uppuganti, S., Nyman, J.S., 2016. Prevalent role of porosity and osteonal area over mineralization heterogeneity in the fracture toughness of human cortical bone. J. Biomech. 49, 2748–2755. https://doi.org/10.1016/j.jbiomech.2016.06.009.

Hayes, A.F., 2022. Introduction to Mediation, Moderation, and Conditional Process Analysis: A Regression-based Approach. Guilford Publications.

Hofbauer, L.C., Busse, B., Eastell, R., Ferrari, S., Frost, M., Müller, R., Burden, A.M., Rivadeneira, F., Napoli, N., Rauner, M., 2022. Bone fragility in diabetes: novel concepts and clinical implications. Lancet Diabetes Endocrinol. 10, 207–220. https://doi.org/10.1016/S2213-8587(21)00347-8.

Jordan, G.R., Loveridge, N., Bell, K.L., Power, J., Rushton, N., Reeve, J., 2000. Spatial clustering of remodeling osteons in the femoral neck cortex: a cause of weakness in hip fracture? Bone 26, 305–313. https://doi.org/10.1016/s8756-3282(99)00272-0.

Khan, M.A.B., Hashim, M.J., King, J.K., Govender, R.D., Mustafa, H., Al Kaabi, J., 2020. Epidemiology of type 2 diabetes - global burden of disease and forecasted trends. J. Epidemiol. Glob. Health 10, 107–111. https://doi.org/10.2991/jegh.k.191028.001.

Khosla, S., Samakkarnthai, P., Monroe, D.G., Farr, J.N., 2021. Update on the pathogenesis and treatment of skeletal fragility in type 2 diabetes mellitus. Nat. Rev. Endocrinol. 17, 685–697. https://doi.org/10.1038/s41574-021-00555-5.

Kusumbe, A.P., Ramasamy, S.K., Adams, R.H., 2014. Coupling of angiogenesis and osteogenesis by a specific vessel subtype in bone. Nature 507, 323–328. https://doi.org/10.1038/nature13145.

Liu, J., Pedoia, V., Heilmeier, U., Ku, E., Su, F., Khanna, S., Imboden, J., Graf, J., Link, T., Li, X., 2016. High-temporospatial-resolution dynamic contrast-enhanced (DCE) wrist MRI with variable-density pseudo-random circular Cartesian undersampling (CIRCUS) acquisition: evaluation of perfusion in rheumatoid arthritis patients. NMR Biomed. 29, 15–23. https://doi.org/10.1002/nbm.3443.

M.T. Löffler, P.-H. Wu, G.J. Kazakia, MR-based techniques for intracortical vessel visualization and characterization: understanding the impact of microvascular disease on skeletal health, Curr. Opin. Endocrinol. Diabetes Obes. (n.d.) doi:https://doi.org/10.1097/MED.0000000000000819.

Ma, L., Oei, L., Jiang, L., Estrada, K., Chen, H., Wang, Z., Yu, Q., Zillikens, M.C., Gao, X., Rivadeneira, F., 2012. Association between bone mineral density and type 2 diabetes mellitus: a meta-analysis of observational studies. Eur. J. Epidemiol. 27, 319–332. https://doi.org/10.1007/s10654-012-9674-x.

Maamari, R.N., Keenan, J.D., Fletcher, D.A., Margolis, T.P., 2014. A mobile phone-based retinal camera for portable wide field imaging. Br. J. Ophthalmol. 98, 438–441. https://doi.org/10.1136/bjophthalmol-2013-303797.

McCalden, R.W., McGeough, J.A., Barker, M.B., Court-Brown, C.M., 1993. Age-related changes in the tensile properties of cortical bone. The relative importance of changes in porosity, mineralization, and microstructure. J. Bone Joint Surg. Am. 75, 1193–1205. https://doi.org/10.2106/00004623-199308000-00009.

McNerny, E.M.B., Nickolas, T.L., 2017. Bone quality in chronic kidney disease: definitions and diagnostics. Curr. Osteoporos. Rep. 15, 207–213. https://doi.org/10.1007/s11914-017-0366-z.

Napoli, N., Chandran, M., Pierroz, D.D., Abrahamsen, B., Schwartz, A.V., Ferrari, S.L., 2017. IOF bone and diabetes working group, mechanisms of diabetes mellitus-induced bone fragility. Nat. Rev. Endocrinol. 13, 208–219. https://doi.org/10.1038/nrendo.2016.153.

Chronic symmetric symptomatic polyneuropathy in the elderly: a field screening investigation in two Italian regions. I. Prevalence and general characteristics of the sample. Italian General Practitioner Study Group (IGPSG). Neurology 45, 1995, 1832–1836. https://doi.org/10.1212/wnl.45.10.1832.

Nirody, J.A., Cheng, K.P., Parrish, R.M., Burghardt, A.J., Majumdar, S., Link, T.M., Kazakia, G.J., 2015. Spatial distribution of intracortical porosity varies across age and sex. Bone 75, 88–95. https://doi.org/10.1016/j.bone.2015.02.006.

Ostertag, A., Peyrin, F., Fernandez, S., Laredo, J.D., de Vernejoul, M.C., Chappard, C., 2014. Cortical measurements of the tibia from high resolution peripheral quantitative computed tomography images: a comparison with synchrotron radiation micro-computed tomography. Bone 63, 7–14. https://doi.org/10.1016/j.bone.2014.02.009.

Patsch, J.M., Burghardt, A.J., Yap, S.P., Baum, T., Schwartz, A.V., Joseph, G.B., Link, T.M., 2013. Increased cortical porosity in type 2 diabetic postmenopausal women with fragility fractures. J. Bone Miner. Res. Off. J. Am. Soc. Bone Miner. Res. 28, 313–324. https://doi.org/10.1002/jbmr.1763.

Pialat, J.B., Burghardt, A.J., Sode, M., Link, T.M., Majumdar, S., 2012. Visual grading of motion induced image degradation in high resolution peripheral computed tomography: impact of image quality on measures of bone density and micro-architecture. Bone 50, 111–118. https://doi.org/10.1016/j.bone.2011.10.003.

Pop-Busui, R., Boulton, A.J.M., Feldman, E.L., Bril, V., Freeman, R., Malik, R.A., Sosenko, J.M., Ziegler, D., 2017. Diabetic neuropathy: a position statement by the American Diabetes Association. Diabetes Care 40, 136–154. https://doi.org/10.2337/dc16-2042.

Ramchand, S.K., Seeman, E., 2018. The influence of cortical porosity on the strength of bone during growth and advancing age. Curr. Osteoporos. Rep. 16, 561–572. https://doi.org/10.1007/s11914-018-0478-0.

Rothman, K.J., Greenland, S., Lash, T.L., 2008. Modern Epidemiology. Lippincott Williams & Wilkins.

Samakkarnthai, P., Sfeir, J.G., Atkinson, E.J., Achenbach, S.J., Wennberg, P.W., Dyck, P.J., Tweed, A.J., Volkman, T.L., Amin, S., Farr, J.N., Vella, A., Drake, M.T., Khosla, S., 2020. Determinants of bone material strength and cortical porosity in patients with type 2 diabetes mellitus. J. Clin. Endocrinol. Metab. 105, dgaa388. https://doi.org/10.1210/clinem/dgaa388.

Samelson, E.J., Demissie, S., Cupples, L.A., Zhang, X., Xu, H., Liu, C.-T., Boyd, S.K., McLean, R.R., Broe, K.E., Kiel, D.P., Bouxsein, M.L., 2018. Diabetes and deficits in cortical bone density, microarchitecture, and bone size: Framingham HR-pQCT study. J. Bone Miner. Res. Off. J. Am. Soc. Bone Miner. Res. 33, 54–62. https://doi.org/10.1002/jbmr.3240.

Schaffler, M.B., Burr, D.B., 1988. Stiffness of compact bone: effects of porosity and density. J. Biomech. 21, 13–16. https://doi.org/10.1016/0021-9290(88)90186-8.

Shanbhogue, V.V., Hansen, S., Frost, M., Jørgensen, N.R., Hermann, A.P., Henriksen, J.E., Brixen, K., 2016. Compromised cortical bone compartment in type 2 diabetes mellitus patients with microvascular disease. Eur. J. Endocrinol. 174, 115–124. https://doi.org/10.1530/EJE-15-0860.

Vercauteren, T., Pennec, X., Perchant, A., Ayache, N., 2009. Diffeomorphic demons: efficient non-parametric image registration. NeuroImage 45, S61–S72. https://doi.org/10.1016/j.neuroimage.2008.10.040.

Vilaca, T., Paggiosi, M., Walsh, J.S., Selvarajah, D., Eastell, R., 2021. The effects of type 1 diabetes and diabetic peripheral neuropathy on the musculoskeletal system: a case-control study. J. Bone Miner. Res. Off. J. Am. Soc. Bone Miner. Res. 36, 1048–1059. https://doi.org/10.1002/jbmr.4271.

Wölfel, E.M., Jähn-Rickert, K., Schmidt, F.N., Wulff, B., Mushumba, H., Sroga, G.E., Püschel, K., Milovanovic, P., Amling, M., Campbell, G.M., Vashishth, D., Busse, B., 2020. Individuals with type 2 diabetes mellitus show dimorphic and heterogeneous patterns of loss in femoral bone quality. Bone 140, 115556. https://doi.org/10.1016/j.bone.2020.115556.

Wu, P.-H., Gibbons, M., Foreman, S.C., Carballido-Gamio, J., Han, M., Krug, R., Liu, J., Link, T.M., Kazakia, G.J., 2019. Cortical bone vessel identification and quantification on contrast-enhanced MR images. Quant. Imaging Med. Surg. 9, 928–941. https://doi.org/10.21037/qims.2019.05.23.

Zimmermann, E.A., Schaible, E., Bale, H., Barth, H.D., Tang, S.Y., Reichert, P., Busse, B., Alliston, T., Ager, J.W., Ritchie, R.O., 2011. Age-related changes in the plasticity and toughness of human cortical bone at multiple length scales. Proc. Natl. Acad. Sci. USA 108, 14416–14421. https://doi.org/10.1073/pnas.1107966108.